

Tumor Cell Kill by c-MYC Depletion: Role of MYC-Regulated Genes that Control DNA Double-Strand Break Repair

Kaisa R. Luoto¹, Alice X. Meng¹, Amanda R. Wasylishen^{1,2}, Helen Zhao¹, Carla L. Coackley¹, Linda Z. Penn^{1,2}, and Robert G. Bristow^{1,2,3}

Abstract

MYC regulates a myriad of genes controlling cell proliferation, metabolism, differentiation, and apoptosis. MYC also controls the expression of DNA double-strand break (DSB) repair genes and therefore may be a potential target for anticancer therapy to sensitize cancer cells to DNA damage or prevent genetic instability. In this report, we studied whether MYC binds to DSB repair gene promoters and modulates cell survival in response to DNA-damaging agents. Chromatin immunoprecipitation studies showed that MYC associates with several DSB repair gene promoters including *Rad51*, *Rad51B*, *Rad51C*, *XRCC2*, *Rad50*, *BRCA1*, *BRCA2*, *DNA-PKcs*, *XRCC4*, *Ku70*, and *DNA ligase IV*. Endogenous MYC protein expression was associated with increased RAD51 and KU70 protein expression of a panel of cancer cell lines of varying histopathology. Induction of MYC in G₀-G₁ and S-G₂-M cells resulted in upregulation of *Rad51* gene expression. MYC knockdown using small interfering RNA (siRNA) led to decreased RAD51 expression but minimal effects on homologous recombination based on a flow cytometry direct repeat green fluorescent protein assay. siRNA to MYC resulted in tumor cell kill in DU145 and H1299 cell lines in a manner independent of apoptosis. However, MYC-dependent changes in DSB repair protein expression were not sufficient to sensitize cells to mitomycin C or ionizing radiation, two agents selectively toxic to DSB repair-deficient cells. Our results suggest that anti-MYC agents may target cells to prevent genetic instability but would not lead to differential radiosensitization or chemosensitization. *Cancer Res*; 70(21); 8748–59. ©2010 AACR.

Introduction

MYC is a basic helix-loop-helix leucine zipper transcription factor that dimerizes with its binding partner MAX and associates with gene promoters containing the E-box motifs CACGTG or CACATG to induce gene transcription (1). MYC controls a broad spectrum of functions including proliferation and cell cycle, differentiation, sensitization to apoptotic stimuli, and genetic instability (1). These functions are deregulated in most human cancers by a variety of mechanisms including gene amplification, insertional mutations, or chromosomal translocation of the *myc* gene. This central role in oncogenesis makes MYC a promising target for stand-alone molecular cancer therapies in cells undergoing oncogene addiction (2). Recent data from Soucek and colleagues (3) have shown that MYC inhibition in a preclin-

ical mouse model of RAS-induced lung adenocarcinoma using a reversible, systemic expression of a MYC mutant that antagonizes MYC activity triggered apoptosis and regression of lung tumors. MYC inhibition exerted profound growth arrest in normal tissues, which were well tolerated (3). This study suggested that targeting MYC could maintain the therapeutic ratio of cancer treatment by preferential killing of tumor cells relative to normal cells. Indeed, anti-MYC agents such as antisense oligonucleotides, small interfering RNA (siRNA), or phosphorodiamidate morpholino oligomers (PMO) have been developed to induce tumor cell growth arrest, differentiation, or apoptosis (4–7).

Previous studies have indicated the association of MYC with the promoters of DNA double-strand break (DSB) repair genes *Nbs1*, *Ku70*, *Rad51*, *BRCA2*, *Rad50*, *Rad54L*, and *DNA-PKcs* (8–11) and the expression of mismatch repair genes (12–14). DSBs are repaired by two major pathways: homologous recombination (HR) and nonhomologous end joining (NHEJ). HR predominates during S and G₂ phases, as it uses sister chromatid in a template-guided manner to repair the DNA break (15). HR relies on the function of RAD51 and its paralogs RAD51B, RAD51C, RAD51D, XRCC2, and XRCC3, as well as BRCA1 and BRCA2 (15). HR-deficient cells are particularly sensitive to the DNA cross-linking agent mitomycin C (MMC). In contrast, NHEJ does not require strand homology and is considered error prone, and it predominates across all phases of the cell cycle. NHEJ requires the action of KU70, KU80, DNA-PKcs, DNA ligase IV, and XRCC4.

Authors' Affiliations: ¹Campbell Family Cancer Research Institute, ²Department of Medical Biophysics, and ³Department of Radiation Oncology, University of Toronto, Radiation Medicine Program, Ontario Cancer Institute/Princess Margaret Hospital, Toronto, Ontario, Canada

Note: Supplementary data for this article are available at Cancer Research Online (<http://cancerres.aacrjournals.org/>).

Corresponding Author: Robert G. Bristow, Radiation Medicine Program, Princess Margaret Hospital, 5th Floor, Room 5-808, 610 University Avenue, Toronto, Ontario, Canada M5G 2M9. Phone: 416-946-2936; Fax: 416-946-4586; E-mail: Robert.Bristow@rmp.uhn.on.ca.

doi: 10.1158/0008-5472.CAN-10-0944

©2010 American Association for Cancer Research.

NHEJ-deficient cells are in turn sensitive to ionizing radiation (IR; ref. 15). Inhibition of MYC-regulated DNA repair could sensitize tumor cells by inducing genetic instability and mitotic catastrophe. Additionally, if MYC regulation of DSB repair gene expression altered chemosensitivity and radiosensitivity, using combinations of MYC inhibitors with DNA-damaging agents could be beneficial. However, few studies have combined molecular targeting of MYC with now standard treatments such as radiochemotherapy or chemotherapy and determined long-term clonogenic cell survival.

Given that MYC promotes genetic instability and has a potential role in DNA repair, we determined whether MYC inhibition leads to decreased DSB repair protein expression and sensitization of tumor cells to IR or MMC (two agents that are selectively toxic to NHEJ- or HR-deficient cancer cells). We show that MYC occupies most DSB repair gene promoters and regulates RAD51 expression. MYC knockdown alone results in loss of long-term clonogenic survival independent of inducing apoptosis. However, partial MYC knockdown, which allowed for colony formation assays, did not further sensitize cells to MMC or IR.

Materials and Methods

Cell culture, generation of inducible MYC cell lines, and siRNA transfections

Normal human diploid fibroblasts GMO5757 (Coriell Cell Repository, 2008) up to 13 passages were used within 6 months of purchase, and cultured as previously described (16). DU145 and PC-3 prostate cancer cells and RKO colon carcinoma cells were obtained from American Type Culture Collection (2001, 2001, and 2007, respectively) and cultured as previously described (17, 18). 22RV1 prostate cancer cells, MCF7 breast cancer cells, Rat-1/*myc* cells, and DR-GFP H1299 lung cancer cells were kind gifts from Drs. Yoni Pinthus (2004; Juravinski Cancer Center, Hamilton, Ontario, Canada), Fei-Fei Liu (2009) and Linda Penn (2001; both at the Ontario Cancer Institute/Princess Margaret Hospital, Toronto, Ontario, Canada), and Simon Powell (2004; Memorial Sloan-Kettering Cancer Center, New York, NY), respectively, and were cultured as described previously (17–22). MCF10A cells were a kind gift from Dr. Senthil Muthuswamy (2003; Ontario Cancer Institute/Princess Margaret Hospital, Toronto, Ontario, Canada) and were cultured as described previously either in full growth medium (23) or in growth factor withdrawal (0.05% horse serum, 10 μ g/mL insulin) to downregulate endogenous MYC. Each cell line was reauthenticated by short tandem repeat (STR) analyses performed by The Centre for Applied Genomics, The Hospital for Sick Children (Toronto, Ontario, Canada; June to September 2010), with the exception of RKO, Rat-1/*myc*, and GMO5757, which lack available STR profiles. The latter cell lines were authenticated by multiple gene expression analyses and comparative genomic hybridization. All cells were tested and found to be *Mycoplasma*-free during experiments.

Inducible pF vector control and pF-MYC cell lines were generated using the 4-hydroxytamoxifen (4-OHT)-inducible

lentiviral expression system as described previously (24). In the presence of 4-OHT, the GEV16 transcription factor controlled by the *Ub* promoter (GEV16-Gal4 DNA-binding domain, estrogen receptor ligand-binding domain, and VP16 transactivation domain) translocates to the nucleus, binds the *5xUAS*, and activates transcription of the gene of interest (24). Briefly, lentiviruses were first generated in 293TV cells. Cells were then infected with viral supernatants in the presence of 0.8 μ g/mL polybrene. Forty-eight hours after infection, stable cell pools were selected in 200 μ g/mL hygromycin and 1 μ g/mL puromycin.

Cells were transfected with Validated Stealth Select RNAi siRNA MYC duplexes 1 or 2 at a concentration of 10 nmol/L in Opti-MEM, or with RAD51 duplexes 1 and 2 at 0.25 nmol/L, or with Stealth RNAi Negative Universal Control using Lipofectamine 2000 (all from Invitrogen) as previously described (17).

Chromatin immunoprecipitation

Chromatin immunoprecipitations (ChIP) were performed essentially as previously described (25) with the following modifications. Nuclei were isolated in 5 mmol/L Tris-HCl (pH 8.0), 85 mmol/L KCl, 0.5% NP40, and 1 \times protease inhibitor cocktail (Roche). Pelleted nuclei were lysed in 50 mmol/L Tris-HCl (pH 8.0), 10 mmol/L EDTA, 1% SDS, and 1 \times protease inhibitor cocktail. Chromatin was sheared to 0.2- to 1.5-kb fragments using a Bioruptor sonicator (Diagenode). Immunoprecipitations were performed in 0.01% SDS, 1.1% Triton X-100, 1.2 mmol/L EDTA, 16.7 mmol/L Tris-HCl (pH 8.0), 167 mmol/L NaCl, and 1 \times protease inhibitor cocktail using the MYC N-262 antibody (Santa Cruz Biotechnology) or rabbit IgG control (Jackson ImmunoResearch Laboratories) with protein A/G beads (Pierce) blocked in 1% bovine serum albumin. DNA was purified using a PCR Purification kit (Qiagen). Immunoprecipitated DNA was amplified using PCR primers (see Supplementary Table S1) *Rad51* (9), *BRCAl* (26), *CAD* (*carbamoyl-phosphate synthetase 2*), and *Chr22* (*chromosome 22*; ref. 9).

Western blotting

Cells were lysed directly in boiling 2 \times SDS buffer [2% SDS, 178 mmol/L Tris-HCl (pH 6.8), 4.5% glycerol]. Protein expression was detected and quantified using primary antibodies MYC (9E10), RAD51 (H-92), KU70 (A-9), and ATM (2C1; Santa Cruz Biotechnology), cyclin D1 (Ab-3; Oncogene), RB (retinoblastoma protein; Pharmingen), α -tubulin (AB-1; Calbiochem), and β -actin (Sigma) and IRDye secondary antibodies with Odyssey IR Imaging System (LI-COR Biosciences).

Reverse transcription and real-time quantitative PCR

RNA was extracted using the RNeasy kit (Qiagen). cDNA was synthesized using the High Capacity cDNA Archive kit (Applied Biosystems). Real-time quantitative PCR was performed in triplicates using the Taqman Gene Expression Assays on a StepOnePlus real-time quantitative PCR instrument (Applied Biosystems). Analysis was performed using the comparative C_t value method.

Cell cycle analysis and fluorescence-activated cell sorting

For cell cycle analysis, cells were treated with 10 $\mu\text{mol/L}$ 5-bromo-2'-deoxyuridine (BrdUrd; Sigma) in culture medium for 1 hour. FITC-conjugated anti-BrdUrd antibody-labeled (BD Biosciences) and propidium iodide (PI)-stained cells were analyzed with a FACSCalibur flow cytometer and CellQuest Pro software (BD Biosciences) as previously described (27). G₀M5757 cell cycle profiles were obtained using PI staining. For cell sorting, MYC expression was induced with 4-OHT for 16 hours in pF-MYC MCF10A cells. Cells were detached by trypsin (Invitrogen) digestion and stained with 10 $\mu\text{g/mL}$ Hoechst 33342 in medium lacking phenol red and supplemented with 10% fetal bovine serum for 90 minutes at 37°C. Cells were sorted into G₀-G₁ and S-G₂-M pools using the MoFlo XDP cell sorter (Beckman Coulter).

Clonogenic survival and apoptosis assays

siRNA-transfected DU145 or H1299 cells were trypsinized after 48 hours and subsequently treated either with 0.5 $\mu\text{g/mL}$ MMC for 1 hour or with 2 Gy IR. Cells were plated in triplicates. The DNA-PKcs inhibitor Ku-0057788 (KuDOS Pharmaceuticals) was used at 1 $\mu\text{mol/L}$ for 1 hour before 2 Gy IR, and medium was changed 16 hours later. For all assays, cells were fixed and stained in 1% methylene blue in 50% ethanol 10 to 15 days later. Surviving clones with >50 cells were scored under a light microscope, and resulting survival was calculated as previously described (27, 28). For apoptosis assays, H1299 cells (or Rat-1/*myc* controls) were treated with 0.5 $\mu\text{g/mL}$ MMC for 1 hour or with 2 or 10 Gy IR at 48 hours after siRNA transfection and assessed for sub-G₁ populations by flow cytometry or nuclear apoptotic bodies, as previously described (21).

HR assay

HR was assessed using a direct repeat green fluorescent protein (DR-GFP) assay essentially as previously described (17). These H1299 cells possess an integrated DR-GFP construct, whose expression is prevented by an insert with the I-SceI restriction site in the reading frame, whereby transfection of I-SceI endonuclease creates a DSB, which when repaired by error-free HR leads to GFP-expressing cells (19, 29). Briefly, H1299 cells were transiently transfected with either the negative control pCMV-1 I-SceI, the functional endonuclease pCMV3xnlI-SceI, or pGFP (as control for transfection efficiency) together with control, MYC, or RAD51 siRNA. Cells were trypsinized 72 hours after transfection and assessed for GFP expression with FACSCalibur flow cytometer and CellQuest Pro software. The percentage of GFP-positive cells in 50,000 to 100,000 events was normalized to the negative control and corrected for transfection efficiency. There were no significant differences in transfection efficiencies between treatments.

Statistical analysis

Statistical analysis was performed using a one-way ANOVA and Tukey's multiple comparison test or a nonlinear curve fit using the Prism 5 software (GraphPad), with $P < 0.05$ con-

sidered significant. Data derived from multiple independent experiments are shown as mean \pm SE.

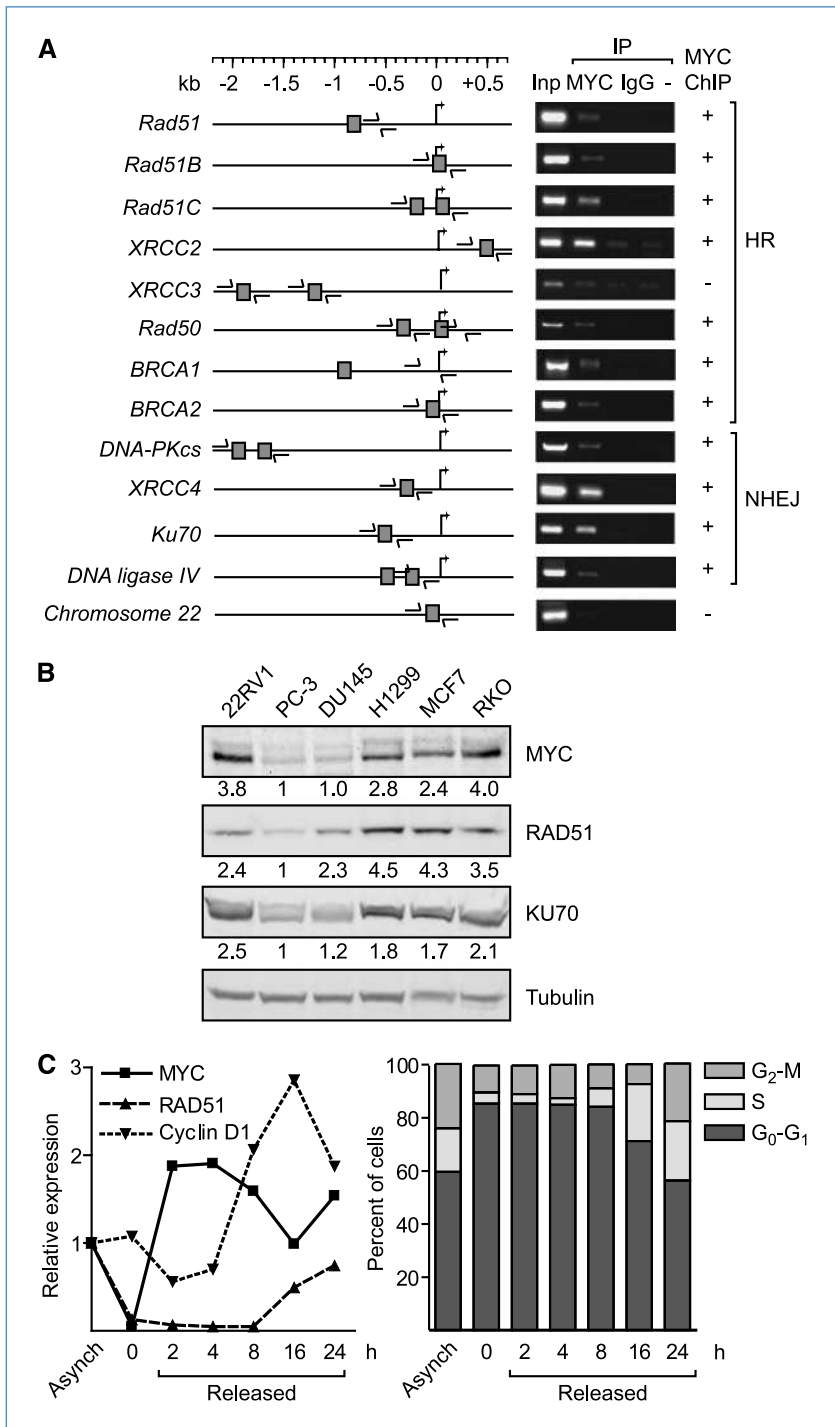
Results

Previous ChIP studies completed by our group showed that MYC can bind the *Rad51* gene promoter (9). We therefore determined whether MYC also binds to other DSB repair gene promoters involved in HR or NHEJ (30–32). *In silico* analyses were performed on sequences spanning from 10 kb upstream to 3 kb downstream of selected DSB repair gene transcription start sites (33). This revealed that there were candidate MYC-binding sites in other DSB repair gene promoter regions (Fig. 1A). To show these interactions *in vivo* using ChIP, we used the prostate cancer cell lines 22RV1, PC-3, and DU145, given our previous publication on their relative HR and NHEJ repair gene expression (34). We focused on candidate sequences nearest to the transcription start sites (Fig. 1A). MYC was found to associate with the majority of the tested HR gene promoters, including *Rad51*, *Rad51B*, *Rad51C*, *XRCC2*, *Rad50*, *BRCAl*, and *BRCAl2* (Fig. 1A; refs. 9–11). Two primer pairs flanking the two most proximal target sequences of *XRCC3* showed weak or no enhanced signal over the negative controls, indicating that MYC was not associated with this promoter region (Fig. 1A). Candidate MYC target sites in NHEJ gene promoters *DNA-PKcs*, *XRCC4*, *Ku70*, and *DNA ligase IV* were all occupied by MYC (Fig. 1A; refs. 10, 11). An E-box motif, not associated with MYC target genes on *Chr22*, was used as a negative control (Fig. 1A; ref. 9). We conclude that MYC can endogenously occupy the promoters of the majority of the DSB repair genes in asynchronously growing cancer cell lines.

Next, we compared the protein expression levels of MYC and two MYC-occupied targets (RAD51 and KU70) in a panel of cell lines with varying histopathology. Endogenous MYC protein expression was associated with increased RAD51 and KU70 protein levels (Fig. 1B). To assess the correlation of MYC and DSB repair protein levels in nontransformed cells, we serum starved normal human fibroblasts G₀M5757 and followed MYC and DSB repair protein expression following serum add back and subsequent cell cycle progression. As expected, MYC protein was negligible in G₀-G₁ cells, but rapidly increased following addition of serum (Fig. 1C; Supplementary Fig. S1). RAD51 was induced on cell cycle progression following cyclin D1 expression (Fig. 1C; Supplementary Fig. S1; ref. 35). These results are consistent with previous observations that MYC and RAD51 protein levels increase with an increase in S-phase fraction (35, 36).

To assess whether MYC is sufficient to activate the expression of DSB repair genes in nontransformed human cells, we generated a stable GEV16-inducible pF-MYC MCF10A cell line (see Materials and Methods; ref. 24). MCF10A cells were grown in medium containing reduced growth factors to downregulate the high levels of endogenous MYC and to dissociate the biological effects of endogenous and 4-OHT-induced exogenous MYC. MYC induction in growth factor-starved cells was sufficient to induce *Rad51* gene expression after 8 hours (Fig. 2A), whereas RAD51 protein expression

Figure 1. MYC association with DSB repair genes. A, candidate MYC target consensus sequences within the promoters of genes involved in HR and NHEJ were validated in ChIP assays using a MYC antibody, rabbit IgG control, or no-antibody control in 22RV1 cells (right). A schematic presentation of DSB repair gene promoters spanning 2 kb from the transcription start site shows candidate MYC target sequences and ChIP primer pairs (arrows). An E-box not targeted by MYC on *Chr22* was used as a negative control. Inp, inputs; IP, immunoprecipitation. B, MYC, RAD51, and KU70 basal protein expression was assessed in 22RV1, PC-3, DU145, H1299, MCF7, and RKO cell lines. Tubulin is shown as a loading control. C, normal human fibroblasts GM05757 were serum starved for 48 h and released into cell cycle by serum stimulation. Cells were harvested 2, 4, 8, 16, and 24 h later. Left, protein expression of MYC, RAD51, and cyclin D1 is presented as normalized to tubulin expression; right, cell cycle profiles obtained by PI staining are presented as mean of four independent experiments. Asynch, asynchronous.



was upregulated after 16 hours (Fig. 2B). MYC induction also resulted in a modest upregulation of *Rad51C*, whereas it had little effect on NHEJ gene expression (Fig. 2A). RB phosphorylation status and cell cycle analyses showed that induction of MYC was associated with S-phase entry only after 16 hours after induction (Fig. 2C). In contrast, *Rad51* gene expression increased at 8 hours before S-phase progression (Fig. 2A

and C). To further eliminate cell cycle bias, we flow sorted pF-MYC cells into G₀-G₁ and S-G₂-M pools followed by protein and RNA analyses. MYC was upregulated in both G₀-G₁ and S-G₂-M phases after 16 hours of induction (Fig. 2D), and RAD51 could be induced in G₀-G₁ cells and was already increased in S-G₂-M cells, independent of MYC (Fig. 2D). *Cyclin A2* mRNA controls were selectively induced in S-G₂-M

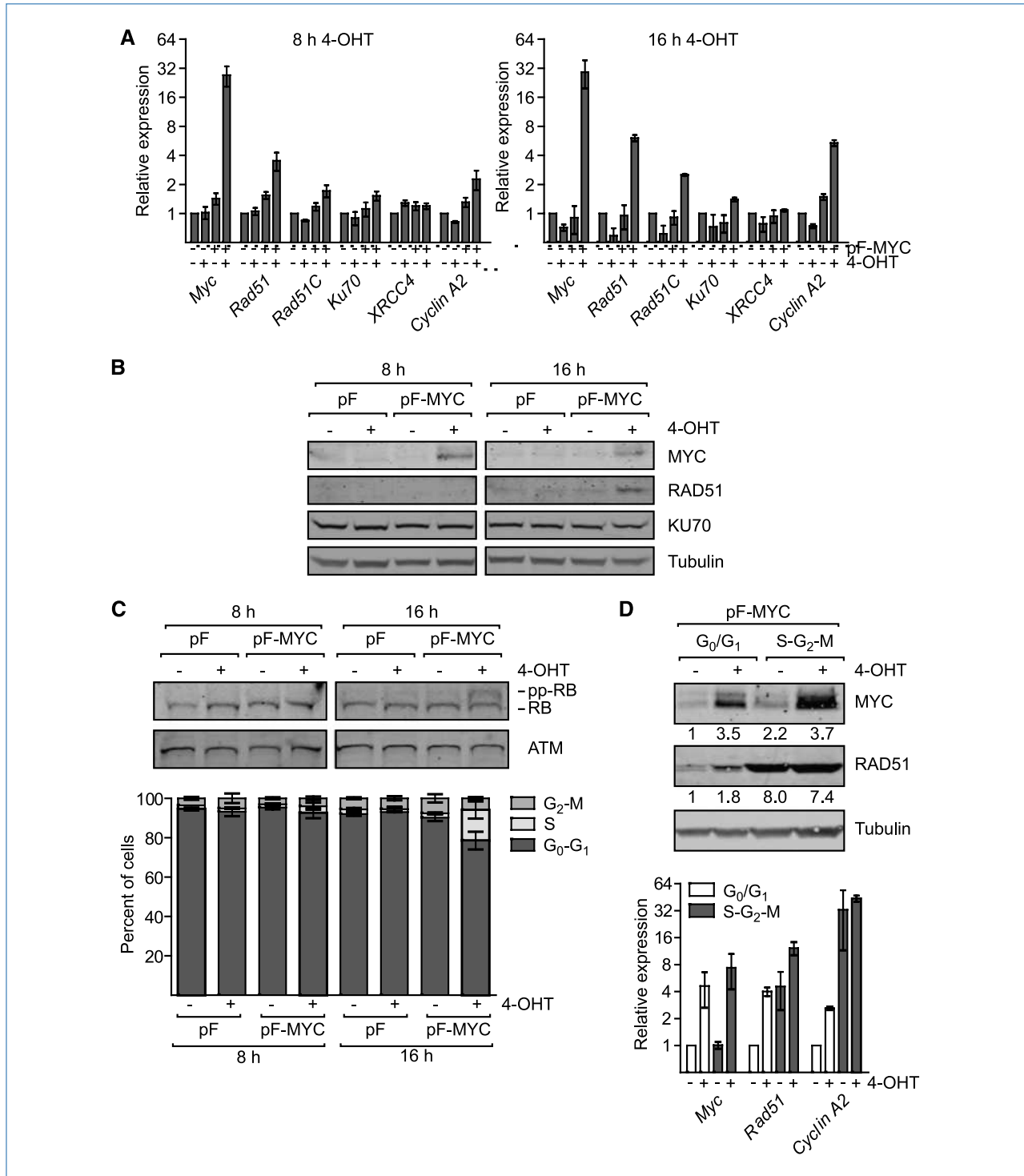


Figure 2. MYC induces *Rad51* expression in nontransformed cells. A to C, inducible pF vector control or pF-MYC MCF10A cells were cultured in growth factor withdrawal for 24 h. Cells were treated with ethanol as a vehicle control or induced with 100 nmol/L 4-OHT for 8 to 16 h. A, *Myc* and DSB repair gene expression at 8 and 16 h after induction is presented relative to *B2M* and normalized to vehicle-treated pF control cells. B, MYC, RAD51, and KU70 protein expression under conditions in A. Tubulin is shown as a loading control. C, hyperphosphorylated RB protein (see top band after induction) and dual-parameter (BrdUrd-Pi) flow cytometry indicates S-phase entry at 16 h after MYC induction. ATM is used as a high-molecular weight loading control. D, pF-MYC cells were vehicle treated or induced by 100 nmol/L 4-OHT for 16 h before fluorescence-activated cell sorting into G₀-G₁ and S-G₂-M pools, followed by protein and RNA analysis. Tubulin is shown as a loading control for Western blotting. *Myc*, *Rad51*, and *cyclin A2* gene expression is presented relative to *B2M* and normalized to the vehicle control at G₀-G₁. Columns, mean of two to three independent experiments; bars, SE.

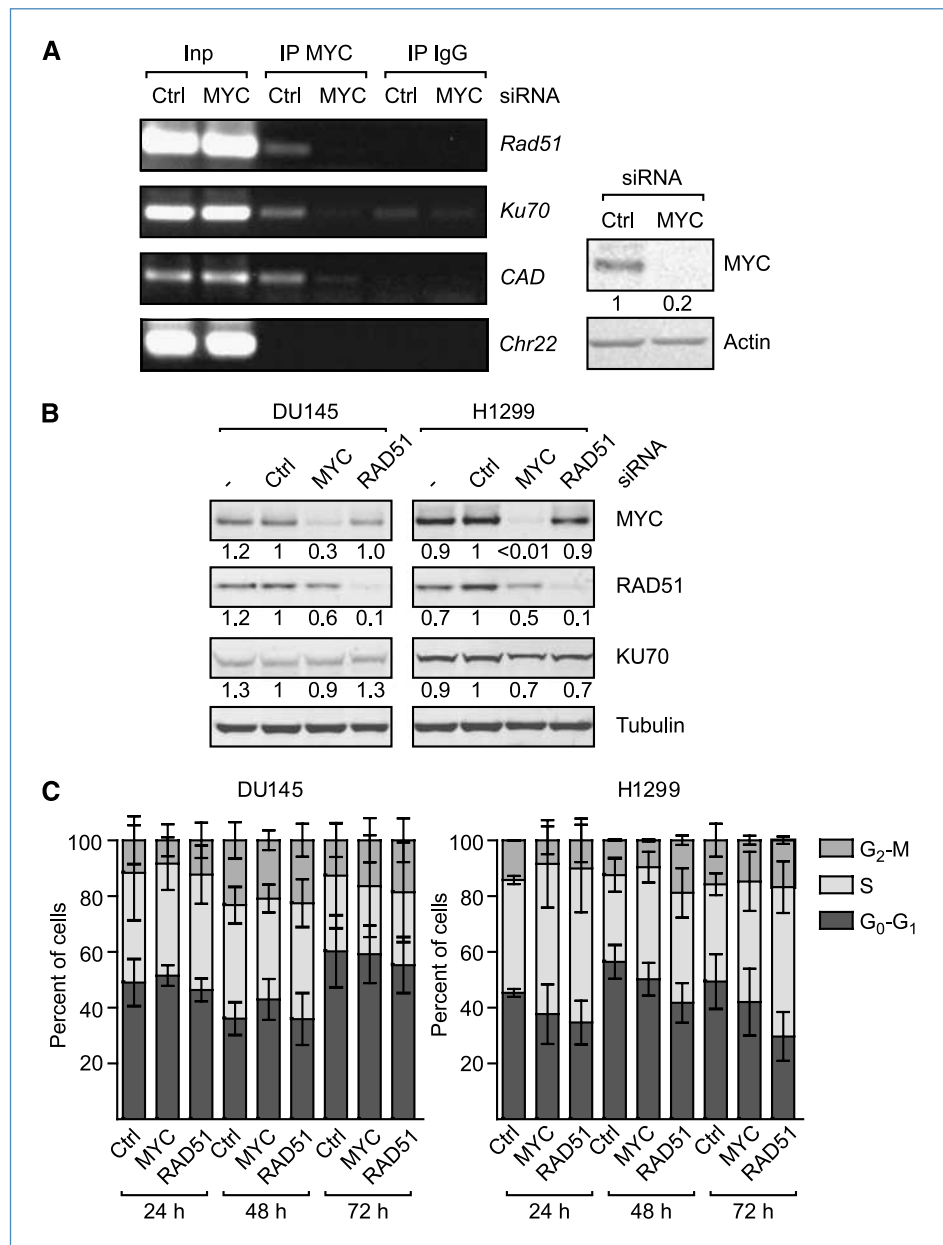
(Fig. 2D; ref. 37). Collectively, these data indicated that MYC can regulate *Rad51* gene and protein expression in G_0 - G_1 nontransiting cells and during G_1 to S cell cycle progression; additional factors in addition to MYC may control *Rad51* expression in S phase.

To determine if MYC occupancy of the *Rad51* promoter was functionally important in cells with downregulated MYC, we characterized the level of MYC and DSB repair gene promoter binding and protein expression following siRNA to MYC. We used DU145 and H1299 cell lines, which express low and high endogenous MYC, respectively, and have detectable endogenous levels of RAD51 protein (see Fig. 1B). MYC-ChIP specificity was confirmed with MYC siRNA, which

resulted in reduced MYC occupation on *Rad51* and *Ku70* gene promoters (Fig. 3A). *CAD* was used as a positive MYC target control, whereas *Chr22* was used as a negative control (Fig. 3A; ref. 9).

Next, we determined the effect of MYC knockdown on DSB repair protein expression. We used an optimal siRNA concentration such that MYC protein levels were reduced to its greatest extent and the control siRNA had the least toxicity (data not shown). MYC siRNA (10 nmol/L) resulted in 60% to 90% reduction of MYC expression and in reduced RAD51 protein levels in DU145 and H1299 cells (Figs. 3B, 5, and 7). In contrast, KU70 protein levels were changed minimally by similar treatment (Fig. 3B), consistent with the lack of

Figure 3. MYC regulates RAD51 in malignant cells. A, H1299 cells were transfected with control (Ctrl) or MYC siRNA (10 nmol/L) and harvested for ChIP assays 48 h later. Occupation of MYC on *Rad51* and *Ku70* promoters was investigated using a MYC antibody or rabbit IgG control. *CAD* was used as a positive MYC target control. An E-box not targeted by MYC on *Chr22* was used as a negative control. Right, fractions of the ChIP cell lysates were analyzed for MYC expression by Western blotting. Actin is shown as a loading control. DU145 and H1299 cells were transfected with control, MYC (10 nmol/L), or RAD51 (0.25 nmol/L) siRNA and harvested 48 h later for protein (B) and 24 to 72 h later for cell cycle (C) analyses. Cell cycle profiles obtained using dual-parameter (BrdUrd-Pi) flow cytometry are presented as a mean of two to four independent experiments. Bars, SE.



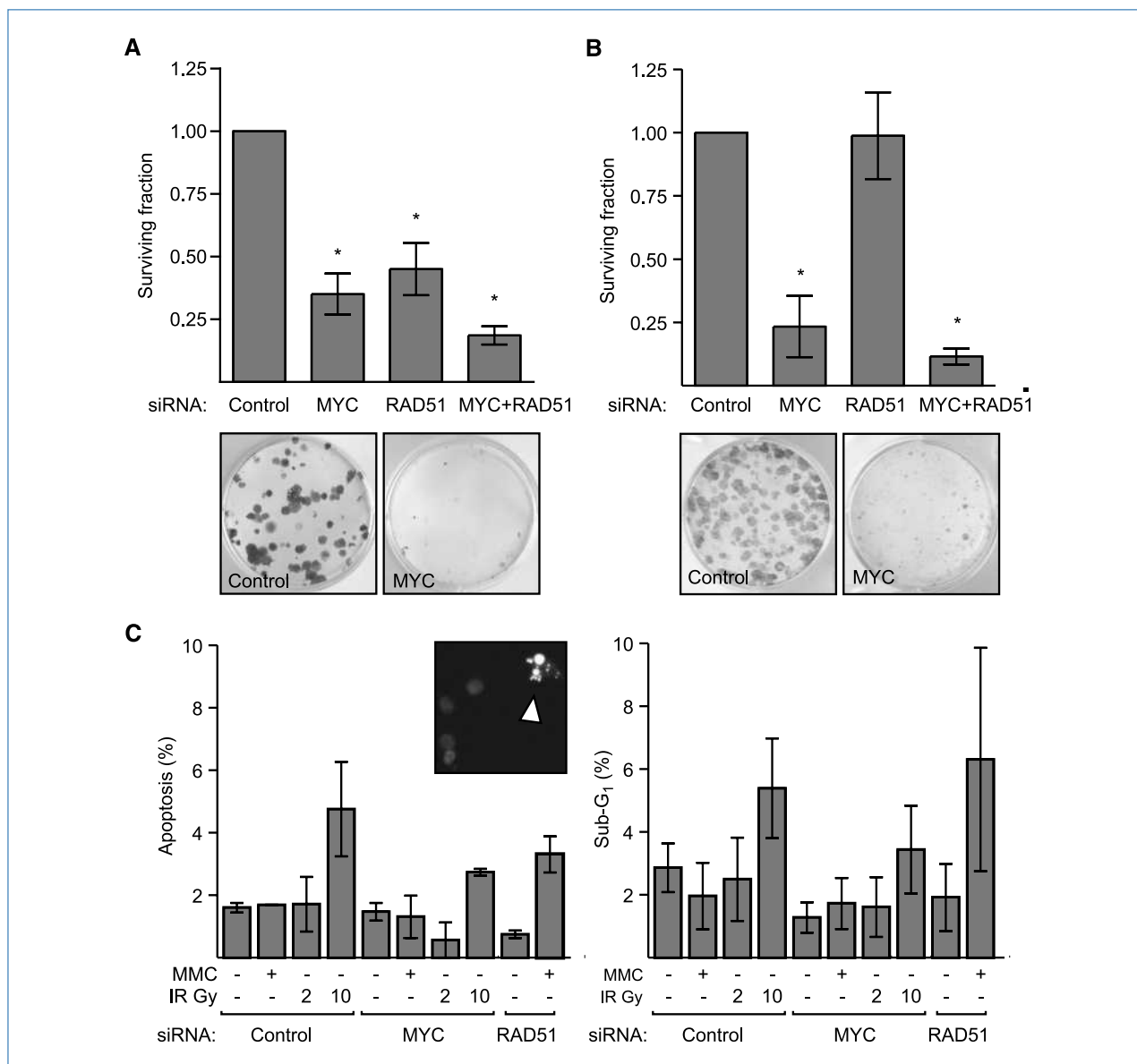


Figure 4. MYC is necessary for cell survival. DU145 (A) and H1299 (B) cells were transfected with control, MYC (10 nmol/L), or RAD51 (0.25 nmol/L) siRNA and plated for colony-forming assays 48 h after treatment. MYC siRNA reduced both surviving cell colony number and size. C, apoptosis was assessed in H1299 cells transfected as in B. Forty-eight hours after transfection, cells were treated with MMC and 2 or 10 Gy IR. Left, apoptotic morphology was determined 72 h after DNA damage using Hoechst 33342 staining; right, sub-G₁ cell populations were assessed 72 h after DNA damage using PI staining. Columns, mean of 2 to 14 independent experiments for each cell line; bars, SE. *, $P < 0.05$.

MYC-dependent *Ku70* expression (Fig. 2A). Next, using the same conditions of MYC siRNA, cell cycle distribution was determined. MYC knockdown resulted in a nonsignificant increase in G₁ fraction in DU145 cells at 24 and 48 hours, and in an inhibition of S-phase progression in H1299 (Fig. 3C). However, we observed reduced proliferation of MYC knockdown DU145 cells in growth assays at later time points (Supplementary Fig. S2). We conclude that MYC-dependent reduction in RAD51 expression is not solely a consequence of a G₁ arrest and that MYC knockdown directly inhibits RAD51, but not KU70, protein expression.

Given the effect of MYC on RAD51 expression, we next performed colony-forming assays to investigate whether modifying MYC or RAD51 would affect long-term clonogenic cell survival based on inhibited RAD51 expression. The survival of DU145 or H1299 cells was not significantly affected by control siRNA transfection (data not shown). We observed decreased cell survival by 65% in DU145 cells and by 77% in H1299 cells following MYC siRNA (Fig. 4A and B). In contrast, RAD51 knockdown resulted in 55% reduced survival in DU145, but did not affect survival in H1299 cells (Fig. 4A and B). The combination of MYC and RAD51 knockdown

resulted in a trend toward additive cell kill in both cell lines (Fig. 4A and B). In addition to reducing the number of surviving cells, MYC siRNA led to smaller surviving colony sizes in both cell lines (Fig. 4A and B). This suggests inhibited growth rate and/or postmitotic cell death of the daughter cells within a colony, and is consistent with DU145 reduced growth rate (Supplementary Fig. S2). MYC downregulation has previously been shown to promote apoptosis (3, 12), and given that siRNA to MYC was more toxic in H1299 cells, we determined whether apoptosis was the mode of cell death in this cell system (Fig. 4C). MYC knockdown alone or combined with DSB-inducing agents did not induce apoptosis as measured by nuclear morphology (Hoechst 33342 staining) or sub-G₁ peak analysis (flow cytometry; Fig. 4C) compared with the positive control, Rat-1/*myc* cells (Supplementary Fig. S3). This indicates that cell death following siRNA to MYC can involve modes of cell death other than apoptosis, as previously documented in irradiated prostate cancer cell lines (21).

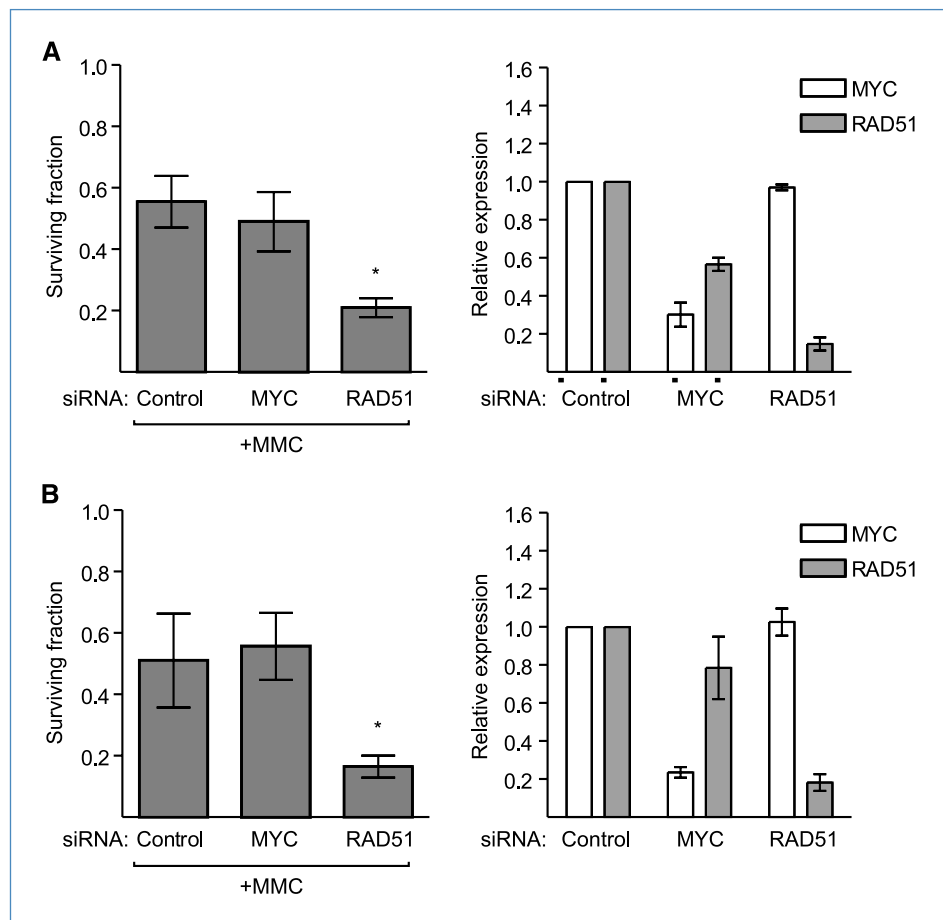
MMC causes intrastrand DNA cross-links that lead to collapsing replication forks and generation of DSBs that are typically repaired by HR (38). We performed colony-forming assays using a combination of MYC siRNA and MMC to see whether MYC knockdown cells were sensitive to HR-

specific agent. An average of 70% knockdown of MYC expression in DU145 cells led to 40% reduction in RAD51, but this was not sufficient to enhance MMC toxicity (Fig. 5A). Consistent with this observation, an average of 80% MYC knockdown in MMC-treated H1299 cells did not result in further cell kill (Fig. 5B). In contrast, RAD51 knockdown resulted in significant MMC sensitivity in both cell lines (Fig. 5). These observations suggest that RAD51, but not MYC, plays a role in the cellular MMC sensitivity of tumor cell clonogens.

Additionally, we performed DR-GFP assays (17) that directly measure HR function (see Materials and Methods; Fig. 6A) to ascertain MYC involvement in functional HR. H1299 cells were cotransfected with the *I-SceI* endonuclease and either control, MYC, or RAD51 siRNA. Cells were harvested 72 hours after transfection to allow sufficient recombination to occur. Whereas RAD51 knockdown reduced HR by 85%, MYC knockdown decreased HR by only 14% (Fig. 6B and C). This was independent of cell cycle following siRNA treatment (Fig. 3C). The mild effect of MYC inhibition on HR may therefore explain the lack of MMC-induced cell kill in MYC knockdown cells.

Finally, we investigated the role of MYC knockdown in cell kill following DSBs induced by IR. Cells deficient in HR or NHEJ will be sensitized to IR treatment (15). Neither

Figure 5. MYC downregulation does not sensitize cells to MMC. DU145 (A) and H1299 (B) cells were transfected with control, MYC (10 nmol/L), or RAD51 (0.25 nmol/L) siRNA for 48 h. Cells were treated with 0.5 μ g/mL MMC and plated for clonogenic survival assays. Columns, mean survival of two to seven independent experiments for each cell line; bars, SE. A and B, right, mean MYC and RAD51 protein expression on Western blots and quantifications collected in parallel to clonogenic assays. *, $P < 0.05$.



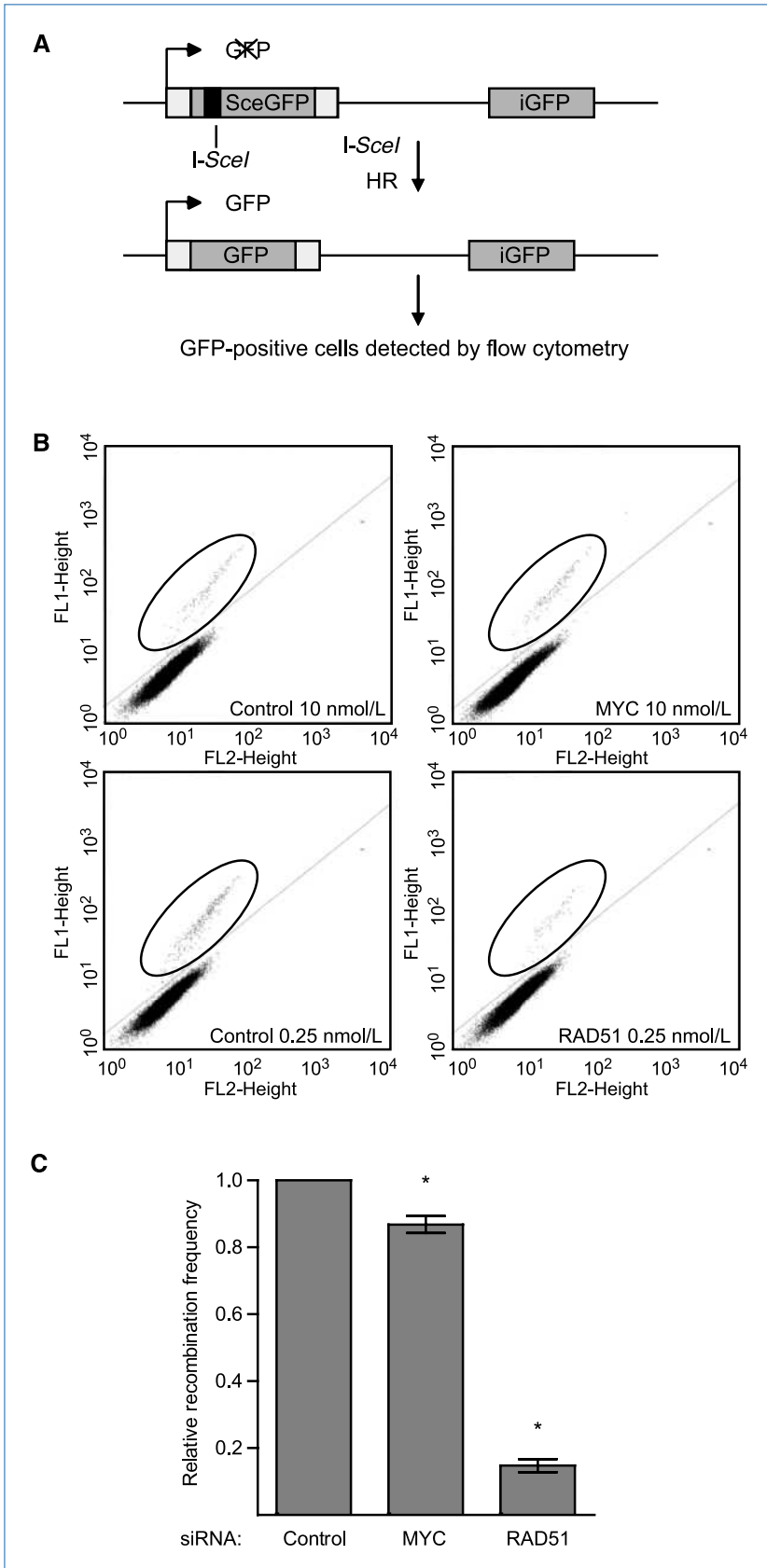
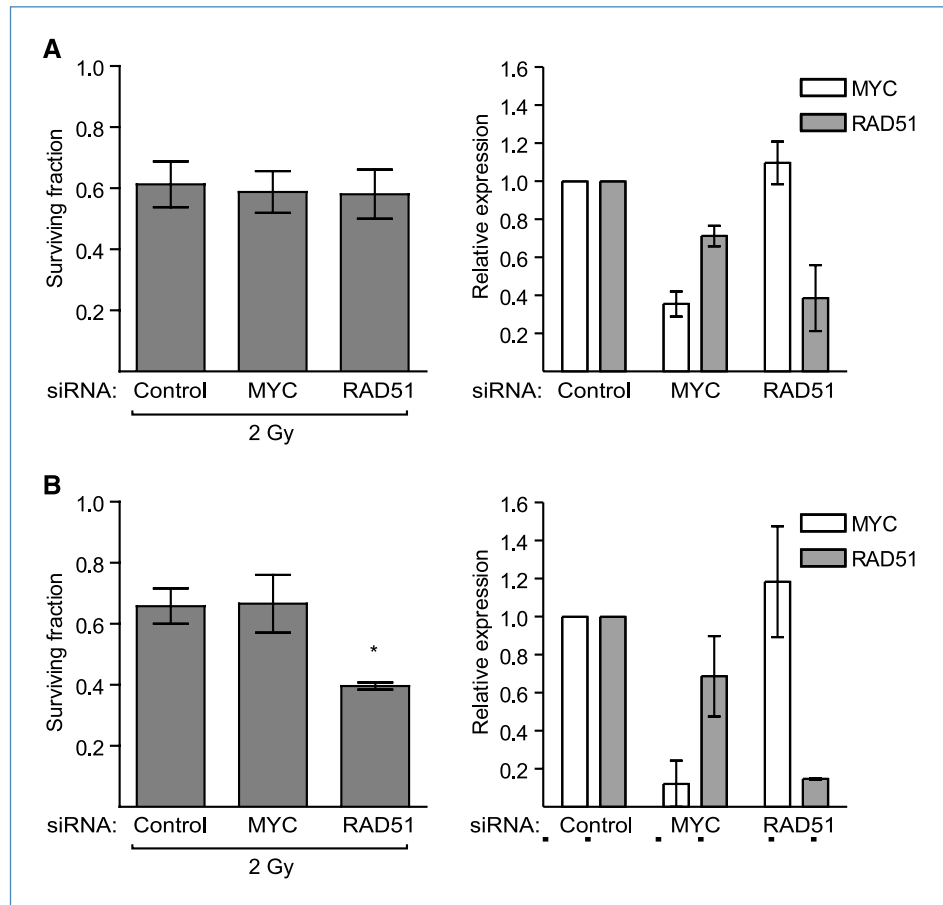


Figure 6. The effect of MYC downregulation on HR. A, H1299 cells that possess a DR-GFP reporter construct express GFP after I-SceI endonuclease cleavage and repair by functional cellular HR. This restores the reading frame and results in GFP expression, which is detected by flow cytometry. B, I-SceI endonuclease expression vector was transfected together with control, MYC (10 nmol/L), or RAD51 (0.25 nmol/L) siRNA. Recombination was analyzed by flow cytometry 72 h after transfection. Representative dot plots are shown. Cells that have undergone HR are circled. C, MYC knockdown led to minor suppression of HR. RAD51 siRNA was used as a positive control. Columns, mean of three independent experiments; bars, SE. *, $P < 0.05$.

Figure 7. MYC knockdown does not sensitize cells to IR. DU145 (A) and H1299 (B) cells were transfected with control, MYC (10 nmol/L), or RAD51 (0.25 nmol/L) siRNA. Forty-eight hours after transfection, cells were plated for clonogenic survival assays and subjected to 2 Gy IR. Columns, mean survival of two to four independent experiments for each cell line; bars, SE. Right, mean MYC and RAD51 protein expression and quantifications completed in parallel to clonogenic assays. *, $P < 0.05$.



DU145 nor H1299 cells exhibited sensitization to a clinically relevant dose of 2 Gy following MYC knockdown (Fig. 7). This is in contrast to the profound radiosensitization of the same cells through inhibition of the NHEJ protein, DNA-PKcs (Supplementary Fig. S4). RAD51 knockdown led to radiosensitization in H1299, but not in DU145, cells (Fig. 7), consistent with the variable IR sensitivity of HR-deficient cells (15). These results indicate that MYC knockdown does not lead to cellular radiosensitization.

Discussion

Previous ChIP array studies have shown the association of MYC to several DSB repair promoters (9–11), and we now report the novel findings that MYC directly transactivates *Rad51* and associates with the Ku70 promoter with little effect on KU70 expression. The MYC-dependent differential regulation of HR versus NHEJ proteins is unknown, but may be a result of differential translational control and protein half-life (17). We also observed that knockdown of MYC leads to inhibition of RAD51, a central factor in HR. Yet, this downregulation was not sufficient to sensitize cells to DNA-damaging agents such as MMC and IR, which preferentially kill HR-deficient cells. MYC has been estimated to regulate 10% to 15% of human genes (10, 11, 33). Global MYC ChIP

array data combined with gene expression data revealed that a vast majority of MYC-associated targets did not change expression following ectopic MYC expression in B cells (33). It has also been speculated that MYC amplification in tumor cells may bind low-affinity E boxes that would be out of its physiologic target range in normal cells (10, 33, 39). Together, these data show the importance of comparing gene and protein expression data with functional assays to ascertain the cell biology associated with MYC promoter binding.

Our results show that under conditions that allow sufficient cell proliferation and clonogenic potential, 60% to 80% reduction of MYC levels alone caused substantial cell death. Targeting MYC by overexpression, antisense, siRNA, inhibitors, or a dominant-interfering MYC mutant can induce apoptosis and growth delay, resulting in tumor regression (2, 3, 40, 41). However, whereas apoptosis does not necessarily affect long-term cell survival (21), fewer studies have shown the effect of MYC inhibition in cellular radiosensitization or chemosensitization in colony-forming survival assays. As such, the 65% to 77% cell kill we observed following MYC siRNA was not explained by apoptotic cell death, as MYC siRNA alone or its combination with MMC or IR did not induce apoptosis. Additionally, MYC-addicted tumor cells can differentiate, senesce, or cease to proliferate on MYC inactivation (42), and highlight the importance of assessing the

efficacy of possible therapeutic applications using long-term clonogenic potential. There are inconsistent conclusions from studies comparing cellular sensitivity with MYC depletion or overexpression, and the outcome may be cell type dependent. Studies have reported NHEJ repair, mismatch repair, and disparate chemotherapy-induced apoptosis or proliferation in the context of both increased and decreased MYC expression in differing tumor cell lines (12, 43–46). We conclude that attempts to combine MYC-related effects in DSB repair gene expression with chemotherapy or radiotherapy may not lead to sensitization of tumor clonogens.

Reducing RAD51 expression by 80–90% resulted in MMC and IR sensitivity in H1299 cells and in MMC sensitivity in DU145 cells. RAD51 is overexpressed in several cancers, and increased levels of RAD51 correlate with increased erroneous recombination and resistance to DNA-damaging agents (47). Given that HR-deficient cells are sensitive to therapies such as MMC, cisplatin, and IR, targeting RAD51 and thereby inhibiting HR is a potential target for combined therapies. For example, imatinib leads to decreased RAD51 expression. Combining imatinib with IR resulted in decreased clonogenic survival *in vitro*, as well as in tumor growth delay in PC-3 prostate cancer xenografts (28). Hence, directly targeting the key players in HR may provide a potent tool for tumor cell radiosensitization, given that indirect HR targeting through MYC did not lead to enhanced sensitivity.

In conclusion, our work suggests that although MYC occupies the majority of DSB repair promoters and controls RAD51 expression, MYC downregulation by siRNA is not sufficient to induce cellular radiosensitivity and MMC sensitivity. However, MYC depletion can lead to cell death directly. Small molecules and PMO as single agents that are not limited by transfection-based methods should be further assessed, as such a strategy may directly target cell proliferation, tumor progression, and genetic instability.

Disclosure of Potential Conflicts of Interest

No potential conflicts of interest were disclosed.

Acknowledgments

We thank Gaetano Zafarana for helpful discussions.

Grant Support

Terry Fox Foundation Program grant 15004, CCSRI Operating grants 17154 and 18298, and Canadian Foundation for Innovation grant to the STTARR Innovation Facility. This research was funded in part by the Ontario Ministry of Health and Long Term Care. The views expressed do not necessarily reflect those of the Ontario Ministry of Health and Long Term Care.

The costs of publication of this article were defrayed in part by the payment of page charges. This article must therefore be hereby marked *advertisement* in accordance with 18 U.S.C. Section 1734 solely to indicate this fact.

Received 03/16/2010; revised 07/12/2010; accepted 08/08/2010; published OnlineFirst 10/12/2010.

References

- Meyer N, Penn LZ. Reflecting on 25 years with MYC. *Nat Rev Cancer* 2008;8:976–90.
- Ponzielli R, Katz S, Baryshte-Lovejoy D, Penn LZ. Cancer therapeutics: targeting the dark side of Myc. *Eur J Cancer* 2005;41:2485–501.
- Soucek L, Whitfield J, Martins CP, et al. Modelling Myc inhibition as a cancer therapy. *Nature* 2008;455:679–83.
- Holt JT, Redner RL, Nienhuis AW. An oligomer complementary to c-myc mRNA inhibits proliferation of HL-60 promyelocytic cells and induces differentiation. *Mol Cell Biol* 1988;8:963–73.
- Kimura S, Maekawa T, Hirakawa K, Murakami A, Abe T. Alterations of c-myc expression by antisense oligodeoxynucleotides enhance the induction of apoptosis in HL-60 cells. *Cancer Res* 1995;55:1379–84.
- Wang YH, Liu S, Zhang G, et al. Knockdown of c-Myc expression by RNAi inhibits MCF-7 breast tumor cells growth *in vitro* and *in vivo*. *Breast Cancer Res* 2005;7:R220–8.
- Iversen PL, Arora V, Acker AJ, Mason DH, Devi GR. Efficacy of antisense morpholino oligomer targeted to c-myc in prostate cancer xenograft murine model and a phase I safety study in humans. *Clin Cancer Res* 2003;9:2510–9.
- Chiang YC, Teng SC, Su YN, Hsieh FJ, Wu KJ. c-Myc directly regulates the transcription of the NBS1 gene involved in DNA double-strand break repair. *J Biol Chem* 2003;278:19286–91.
- Mao DY, Watson JD, Yan PS, et al. Analysis of Myc bound loci identified by CpG island arrays shows that Max is essential for Myc-dependent repression. *Curr Biol* 2003;13:882–6.
- Fernandez PC, Frank SR, Wang L, et al. Genomic targets of the human c-Myc protein. *Genes Dev* 2003;17:1115–29.
- Li Z, Van Calcar S, Qu C, Cavenee WK, Zhang MQ, Ren B. A global transcriptional regulatory role for c-Myc in Burkitt's lymphoma cells. *Proc Natl Acad Sci U S A* 2003;100:8164–9.
- Bucci B, D'Agnano I, Amendola D, et al. Myc down-regulation sensitizes melanoma cells to radiotherapy by inhibiting MLH1 and MSH2 mismatch repair proteins. *Clin Cancer Res* 2005;11:2756–67.
- Bindra RS, Glazer PM. Co-repression of mismatch repair gene expression by hypoxia in cancer cells: role of the Myc/Max network. *Cancer Lett* 2007;252:93–103.
- Menssen A, Hermeking H. Characterization of the c-MYC-regulated transcriptome by SAGE: identification and analysis of c-MYC target genes. *Proc Natl Acad Sci U S A* 2002;99:6274–9.
- Bristow RG, Ozcelik H, Jalali F, Chan N, Vesprini D. Homologous recombination and prostate cancer: a model for novel DNA repair targets and therapies. *Radiother Oncol* 2007;83:220–30.
- Al Rashid ST, Dellaire G, Cuddihy A, et al. Evidence for the direct binding of phosphorylated p53 to sites of DNA breaks *in vivo*. *Cancer Res* 2005;65:10810–21.
- Chan N, Koritzinsky M, Zhao H, et al. Chronic hypoxia decreases synthesis of homologous recombination proteins to offset chemoresistance and radioresistance. *Cancer Res* 2008;68:605–14.
- Meng AX, Jalali F, Cuddihy A, et al. Hypoxia down-regulates DNA double strand break repair gene expression in prostate cancer cells. *Radiother Oncol* 2005;76:168–76.
- Romanova LY, Willers H, Blagosklonny MV, Powell SN. The interaction of p53 with replication protein A mediates suppression of homologous recombination. *Oncogene* 2004;23:9025–33.
- Penn LJ, Brooks MW, Laufer EM, Land H. Negative autoregulation of c-myc transcription. *EMBO J* 1990;9:1113–21.
- Bromfield GP, Meng A, Warde P, Bristow RG. Cell death in irradiated prostate epithelial cells: role of apoptotic and clonogenic cell kill. *Prostate Cancer Prostatic Dis* 2003;6:73–85.
- Ma N, Szmítko P, Brade A, et al. Kinase-dead PKB gene therapy combined with hyperthermia for human breast cancer. *Cancer Gene Ther* 2004;11:52–60.

23. Debnath J, Muthuswamy SK, Brugge JS. Morphogenesis and oncogenesis of MCF-10A mammary epithelial acini grown in three-dimensional basement membrane cultures. *Methods* 2003;30:256–68.
24. Callus BA, Ekert PG, Heraud JE, et al. Cytoplasmic p53 is not required for PUMA-induced apoptosis. *Cell Death Differ* 2008;15:213–5.
25. Milton AH, Khaire N, Ingram L, O'Donnell AJ, La Thangue NB. 14-3-3 proteins integrate E2F activity with the DNA damage response. *EMBO J* 2006;25:1046–57.
26. Bindra RS, Gibson SL, Meng A, et al. Hypoxia-induced down-regulation of BRCA1 expression by E2Fs. *Cancer Res* 2005;65:11597–604.
27. Cuddihy AR, Jalali F, Coackley C, Bristow RG. WTP53 induction does not override MTP53 chemoresistance and radioresistance due to gain-of-function in lung cancer cells. *Mol Cancer Ther* 2008;7:980–92.
28. Choudhury A, Zhao H, Jalali F, et al. Targeting homologous recombination using imatinib results in enhanced tumor cell chemosensitivity and radiosensitivity. *Mol Cancer Ther* 2009;8:203–13.
29. Pierce AJ, Johnson RD, Thompson LH, Jasin M. XRCC3 promotes homology-directed repair of DNA damage in mammalian cells. *Genes Dev* 1999;13:2633–8.
30. Transcriptional regulatory element database. Cold Spring Harbor (NY): Cold Spring Harbor Laboratory; 2008.
31. Schug J. Using TESS to predict transcription factor binding sites in DNA sequence. *Curr Protoc Bioinformatics* 2008;Chapter 2:Unit 2.6.
32. Heinemeyer T, Wingender E, Reuter I, et al. Databases on transcriptional regulation: TRANSFAC, TRRD and COMPEL. *Nucleic Acids Res* 1998;26:362–7.
33. Zeller KI, Zhao X, Lee CW, et al. Global mapping of c-Myc binding sites and target gene networks in human B cells. *Proc Natl Acad Sci U S A* 2006;103:17834–9.
34. Fan R, Kumaravel TS, Jalali F, Marrano P, Squire JA, Bristow RG. Defective DNA strand break repair after DNA damage in prostate cancer cells: implications for genetic instability and prostate cancer progression. *Cancer Res* 2004;64:8526–33.
35. Beier F, Ali Z, Mok D, et al. TGF β and PTHrP control chondrocyte proliferation by activating cyclin D1 expression. *Mol Biol Cell* 2001;12:3852–63.
36. Essers J, Hendriks RW, Wesoly J, et al. Analysis of mouse Rad54 expression and its implications for homologous recombination. *DNA Repair (Amst)* 2002;1:779–93.
37. Zindy F, Lamas E, Chenivesse X, et al. Cyclin A is required in S phase in normal epithelial cells. *Biochem Biophys Res Commun* 1992;182:1144–54.
38. Helleday T, Petermann E, Lundin C, Hodgson B, Sharma RA. DNA repair pathways as targets for cancer therapy. *Nat Rev Cancer* 2008;8:193–204.
39. Freie BW, Eisenman RN. Ratcheting Myc. *Cancer Cell* 2008;14:425–6.
40. Wang H, Mannava S, Grachtchouk V, et al. c-Myc depletion inhibits proliferation of human tumor cells at various stages of the cell cycle. *Oncogene* 2008;27:1905–15.
41. Biliran H, Jr., Banerjee S, Thakur A, et al. c-Myc-induced chemosensitization is mediated by suppression of cyclin D1 expression and nuclear factor- κ B activity in pancreatic cancer cells. *Clin Cancer Res* 2007;13:2811–21.
42. Felsher DW. Reversing cancer from inside and out: oncogene addiction, cellular senescence, and the angiogenic switch. *Lymphat Res Biol* 2008;6:149–54.
43. Karlsson A, Deb-Basu D, Cherry A, Turner S, Ford J, Felsher DW. Defective double-strand DNA break repair and chromosomal translocations by MYC overexpression. *Proc Natl Acad Sci U S A* 2003;100:9974–9.
44. Sklar MD, Prochownik EV. Modulation of *cis*-platinum resistance in Friend erythroleukemia cells by c-myc. *Cancer Res* 1991;51:2118–23.
45. Funato T, Kozawa K, Kaku M, Sasaki T. Modification of the sensitivity to cisplatin with c-myc over-expression or down-regulation in colon cancer cells. *Anticancer Drugs* 2001;12:829–34.
46. von Bueren AO, Shalaby T, Oehler-Janne C, et al. RNA interference-mediated c-MYC inhibition prevents cell growth and decreases sensitivity to radio- and chemotherapy in childhood medulloblastoma cells. *BMC Cancer* 2009;9:10.
47. Klein HL. The consequences of Rad51 overexpression for normal and tumor cells. *DNA Repair (Amst)* 2008;7:686–93.